Article

Inhibition of experimental choroidal neovascularization by a novel peptide derived from calreticulin anti-angiogenic domain

Youn-Shen Bee1,2,3, Yi-Ling Ma4, Jinying Chen5,6, Pei-Jhen Tsai1, Shwu-Jiuan Sheu1,6,7, Hsiu-Chen Lin1, Hu Huang9, Guei-Sheung Liu5,6,10† and Ming-Hong Tai11,12,13,14†

[1]Department of Ophthalmology, Kaohsiung Veterans General Hospital, Kaohsiung, Taiwan
[2]Yuh-Ing Junior College of Health Care & Management, Kaohsiung, Taiwan
[3]National Defense Medical Center, Taipei, Taiwan
[4]Division of Nephrology, Kaohsiung Veterans General Hospital, Kaohsiung, Taiwan
[5]Menzies Institute for Medical Research, University of Tasmania, Hobart, Tasmania, Australia
[6]Department of Ophthalmology, Jinan University, Guangzhou, Guangdong, China
[7]School of Medicine, National Yang-Ming University, Taipei, Taiwan
[8]Department of Medical Education and Research, Kaohsiung Veterans General Hospital, Kaohsiung, Taiwan
[9]Aier Eye Institute; Aier School of Ophthalmology, Central South University, Changsha, Hunan, China
[10]Ophthalmology, Department of Surgery, University of Melbourne, East Melbourne, Victoria, Australia
[11]Department of Biomedical Sciences, National Sun Yat-Sen University, Kaohsiung, Taiwan
[12]Center for Neuroscience, National Sun Yat-Sen University, Kaohsiung, Taiwan
[13]Doctoral Degree Program in Marine, Biotechnology, National Sun Yat-Sen University, Kaohsiung, Taiwan
[14]Graduate Institute of Medicine, Kaohsiung Medical University, Kaohsiung, Taiwan
†These authors contributed equally to this work and should be regarded as equal senior authors.

Running title: Calreticulin-derived peptide inhibits choroidal neovascularization
Correspondence should be addressed to: Guei-Sheung Liu, Ph. D.
Menzies Institute for Medical Research, University of Tasmania. 17 Liverpool Street, Hobart, Hobart, TAS 7000, Australia. Tel: +61-3-62264250, FAX: +61-3-62267704,
e-mail: rickliu0817@gmail.com
and Ming-Hong Tai, Ph. D.
Department of Biomedical Sciences, National Sun Yat-Sen University. No.70, Lianhai Rd., Kaohsiung City 804, Taiwan Tel: +886-7-5252000 ext. 5816, FAX: +886-7-3468054,
e-mail: minghongtai@gmail.com

Abstract: Choroidal neovascularization (CNV) is a key pathological feature of several of the leading causes of vision loss including neovascular age-related macular degeneration. Here we show that a calreticulin anti-angiogenic domain (CAD)-like peptide 27, CAD27, inhibited *in vitro* angiogenic activities, including tube formation and migration of endothelial cells, and suppressed vascular sprouting from rat aortic ring explants. In rat model of laser-induced CNV, we demonstrate that intravitreal injection of CAD27 significantly attenuated the formation of CNV lesions as measured via fundus fluorescein angiography and choroid flat-mounts (19.5% and 22.4% reductions at 10μg and 20μg of CAD27 injected, respectively). Similarly, the reduction of CNV lesions was observed in the groups of rats that had received topical applications of CAD27 (choroid flat-mounts: 17.9% and 32.5% reductions at 10μg/mL and 20μg/mL of CAD27 installed, respectively). Retinal function was unaffected, as measured using electroretinography in both groups received interareal injection or topical applications of CAD27 at least for 9 days. These findings show that CAD27 can be used as a potential therapeutic alternative for targeting CNV in the diseases such as neovascular age-related macular degeneration.

 doi:10.20944/preprints201807.0347.v2

Keywords: choroidal neovascularization; neovascular age-related macular degeneration; calreticulin anti-angiogenic domain

1.introduction

Choroidal neovascularization (CNV) is the primary cause for vision loss in patients with wet (exudative or neovascular) age-related macular degeneration (nAMD; see review in ref[1]) and degenerative myopia (see review in ref[2]). In these conditions, abnormally high levels of vascular endothelial growth factor (VEGF) are secreted. VEGF causes the pathological formation of blood vessels in the eye but also leads to leakage of blood and fluid into the eye, damaging the retina and leading to vision loss. The recent availability of anti-VEGF therapies (VEGF-neutralizing proteins, such as monoclonal antibodies, antibody fragments and antibody-receptor fusion proteins) has revolutionized the treatment of CNV by preserving and even restoring vision in patients[3, 4]. However, existing anti-VEGF therapeutics are expensive and require frequent intravitreal injections (often for many years) to achieve therapeutic benefit. Moreover, a lack of capacity for repeated injections in the public health system may also pose a barrier to access for patients. Thus, there is a need to seek cost-effective and less-invasive and more durable alternative therapies for these conditions.

The calreticulin anti-angiogenic domain (CAD; also known as vasostatin), the N-terminal domain of calreticulin, comprising amino acids 1-180, is a potent endogenous inhibitor of angiogenesis[5]. Recombinant CAD has been shown to inhibit basic fibroblast growth factor (bFGF)- or VEGF-induced angiogenic responses of human endothelial cells[6-8] by preventing attachment of endothelial cells to laminin, thus reducing the angiogenic responses of endothelial cells[9]. CAD also has anti-inflammatory properties, which potentiates its antiangiogenic effects by limiting inflammation-driven angiogenic triggers[10]. Moreover, intramuscular gene delivery or topical application of CAD has been demonstrated to suppress corneal and choroidal neovascularization in rats. Here, we have extended the previously studies to identify the functional domain of CAD into a cyclic peptide fragment of 27 residues, CAD-like peptide 27 (CAD27), which consists of residues 137-163 of calreticulin. We then investigated the anti-angiogenic effect and therapeutic efficacy of CAD27 *in vitro* and *in vivo* in a rat model of laser-induced CNV via intravitreal administration and topical application.

2.Results

2.1.Identify the functional domain of CAD for the inhibition of angiogenesis.

To identify the anti-angiogenic functional fragment of CAD, a stop codon was introduced into the different amino acid sequence of the thioredoxin (TrxA)-CAD48 construct to generate the truncated CAD proteins (T141, N149, I157, D165, and T173) by the site-directed mutagenesis (Figure 1A and B). The recombinant proteins were over-expressed as TrxA-tagged proteins in *Escherichia coli* and purified using Ni-NTA affinity chromatography. The purity of the purified fragments was estimated to be approximately 90% (Figure 1C). We next performed a Boyden's chamber migration assay to examine the effects of the truncated CAD fragments on the angiogenic activity of primary human endothelial cells (HUVECs). As shown Figure 1D, the migration ability of HUVECs was not affected by the treatment of TrxA, TrxA-T141 and TrxA-T149 protein (the number of migrated cells in TrxA: 87±7, n=3; TrxA-T141: 99±14, n=3; TrxA-T149: 70±9, n=3). The migration of HUVECs was significantly reduced by the treatment of TrxA-I157, TrxA-D165 and TrxA-T173 protein (TrxA-I157: 44±13, n=3; TrxA-D165: 33±10, n=3; TrxA-T173: 25±7, n=3). These results suggest that CAD covering 149-165 amino acid is responsible for the inhibition of endothelial cell migration. In addition, we further generated two truncated CAD fragments, CAD27 and CAD36, which consists of residues C137-C162 and C137-Y172 of calreticulin covering the functional motif of CAD and in a cyclic

structure format (Figure 1A and B). Our data showed that TrxA-CAD27 (24±3, n=3) and TrxA-CAD36 (residues C137-Y172; 38±5, n=3) have a comparable function in inhibiting the migration of HUVECs to TrxA-CAD48 (18±2, n=3) (Figure 1D).

2.2.CAD27 inhibits the angiogenic activity of endothelial cells in vitro and vascular sprouting from rat aortic ring ex vivo.

The CAD27 cyclic peptide was manufactured by de novo synthesis for *in vitro* and *in vivo* studies (Figure 2A). To evaluate the anti-angiogenic activity of CAD27 peptides, endothelial tube formation, migration and rat aortic ring assay were performed. Compared with vehicle (the percentage of lumen count: 100±1.5%, n=4) or Csr27-treated cells (Csr27 10 μg/mL: 92.6±2.5%, n=4; and Csr27 20 μg/mL: 99.6±1.3%, n=4), cells treated with CAD27 (CAD27 10 μg/mL: 17.4±2.3%, n=4; and CAD27 20 μg/mL: 1.7±0.8%, n=4) showed a significant decrease in their capacity to form tube-like networks on Matrigel (Figure 2B). Additionally, CAD27-treated cells also showed poorer migration in the Boyden's chamber migration assay (the number of migrated cells in vehicle: 134±9, n=4; Csr27 10 μg/mL: 116±8, n=3; or Csr27 20 μg/mL: 123±2, n=3; compared with CAD27 10 μg/mL: 77±6, n=3; or CAD27 20 μg/mL: 67±5, n=3) (Figure 2C).

To further validate the anti-angiogenic function of CAD27 *ex vivo*, the rat aortic rings were embedded in Matrigel to assess microvascular sprouting. A significant reduction of vessel sprouting from aortic ring was found in the CAD27-treated group (the percentage of sprouting length: 12.2±0.7%, n=5) compared to the vehicle- (100±3.4%, n=5) or Csr27-treated group (89.7±0.9%, n=5) (Figure 3).

2.3.Effect of intravitreal or topical delivery of CAD27 on retinal function in the rat retina

To determine whether employment of CAD27 affects retinal safety, we examined retinal function with ERG on day 14 after CAD27 treatments. There was no statistical difference in the latency and amplitude of the a-wave and b-wave in the eyes with intravitreal injection or topical application of CAD27 compared with the eyes-treated with vehicle or Lucentis (n=12; Table 1 and Supplementary Figure 1). These results indicate that there was no obvious retinal toxicity after intravitreal injection and topical application of CAD27.

2.4.Intravitreal and topical delivery of CAD27 alleviates laser-induced CNV lesions in rats

A rat model of laser-induced CNV was employed to evaluate the therapeutic potential of intravitreal and topical delivery of CAD27. One day after the laser surgery, CAD27 was administered via a single intravitreal injection or daily topical application (three times a day) in the CNV rats. The extent of choroidal vascularization was examined using fundus fluorescein angiography and choroidal flat-mounts with FITC-dextran perfusion on 24 and 28 days respectively after CNV induction (Figure 4A). Compared with vehicle-treated eyes (60% of the eyes had score 3, 33% had score 2, and 7% had score 1, n=42), intravitreal injection of CAD27 (10 μg CAD27: 11% of the eyes had score 3, 52% had score 2, and 37% had score 1, n=27; 20 μg CAD27: 2% of the eyes had score 3, 43% had score 2, and 55% had score 1, n=40) and Lucentis (8% of the eyes had score 3, 46% had score 2, and 46% had score 1, n=26) reduced CNV score measured by FFA on day 24 (Figure 4B and 4C). Similarly, the daily topical application of CAD27 also reduced the CNV score (10 μg/mL CAD27: 2% of the eyes had score 3, 58% had score 2, and 40% had score 1, n=46; 20 μg/mL CAD27: 3% of the eyes had score 3, 30% had score 2, and 67% had score 1, n=44) (Figure 4B and 4C).

To further confirm the therapeutic potential of CAD27, the size of CNV lesion was measured using flat-mount analysis after perfusion with FITC-dextran on day 28 (Figure 5A and Supplementary Figure 2). Compared with vehicle-treated eyes (the CNV size: 82867±4880 [95% CI: 73303-92430] μm^2, n=30), a significant reduction in the size of CNV lesion was found in the rat eyes that had received an intravitreal administration of CAD27 (CAD27 10μg: 66714±2589 [95% CI: 61640-71787, n=31] μm^2 and CAD27 20μg: 64327±2341 [95% CI: 59738-68915, n=23] μm^2) and Lucentis (62233±3050 [95% CI: 56256-68209, n=30] μm^2) as well as daily topical application of CAD27 (CAD27 10μg/mL: 67959±2313 [95% CI: 63425-72492, n=26] μm^2 and CAD27 20μg/mL: 55911±3771 [95% CI:

 doi:10.20944/preprints201807.0347.v2

48519-63302, n=26] μm^2; Figure 5B). These results indicate that intravitreal and topical application of CAD27 attenuated the severity of experimental CNV.

3.Discussion

In present study, we have identified the core antiangiogenic domain of CAD and demonstrated that the de novo synthetic CAD27 cyclic peptides can inhibit angiogenesis *in vitro*, *ex vivo* and suppress ocular neovascularization *in vivo*. Specifically, we have confirmed the anti-angiogenic activity of CAD27 by inhibition of endothelial tube formation and migration, as well as the vascular sprouting from rat aortic ring. Intravitreal and topical application of CAD27 attenuated laser-induced CNV in rats as revealed by using FFA and choroidal flat-mount, and no detectable adverse effects on retinal function was found by ERG.

Treatment for nAMD has recently been revolutionized by the availability of intravitreal anti-VEGF agents[11]. Such agents that bind to VEGF thereby preventing Flt-1 and KDR/Flk-1 signaling and inhibiting the neovascular response have been shown to be superior to previous treatment modalities such as verteporfin photodynamic therapy[12]. While there is promise for improvement in vision with intravitreal anti-VEGF agents, there are also shortcomings in terms of variable response to therapy as well as loss of efficacy in a subgroup of patients. Over the years, many endogenous inhibitors of angiogenesis including various antiangiogenic peptides, hormone metabolites, and apoptosis modulators have been discovered and proposed as potential therapeutic alternatives for targeting neovascularization and/or excessive vascular leakage in the eye[13]. Some of them have reached clinical trial stages including PEDF (ClinicalTrials.gov Identifier: NCT00109499) and endostatin/angiostatin (RetinoStat) (ClinicalTrials.gov Identifier: NCT01678872 and NCT01301443) for the treatment of nAMD. Similar to these endogenous angiogenesis inhibitors, CAD is also a naturally occurring antiangiogenic peptide derived from the human calreticulin. Unlike most of angiogenesis inhibitors appear to have more complex activities, CAD specifically targets proliferating endothelial cells with low toxicity[7, 14, 15]. Moreover, CAD appear to have a 4-10 fold lower effective dose then endostatin and angiostatin for angiogenesis inhibition *in vivo* [16, 17] as well as has anti-inflammatory properties that will help to control inflammation, a major contributor to the ongoing drive for neovascularization in nAMD[10]. These favourable features make CAD superior to previously identified angiogenesis inhibitors are derived from fragments of endogenous precursor proteins as well as current therapeutic approaches (e.g. anti-VEGF antibody injections).

Our previous studies have demonstrated that gene delivery of CAD and its derived fragment (CAD112) can attenuate the development of choroidal and retinal neovascularization in rodent models of laser-induced CNV and oxygen-induced retinopathy[18]. However, adverse effects associated with prolonged expression of vascular targeting proteins by gene delivery may have unwanted side effects, including retinal vascular toxicity. There are also other major obstacles to the acceleration of gene therapy from bench to bedside, such as cost of the treatment[19]. Therefore, in the present study, we rationally designed a small fragment of CAD, CAD27, which covers the core antiangiogenic domain of CAD and can be produced by chemically synthesis at a lower cost than its parent molecule, recombinant CAD protein or CAD gene therapy. Moreover, the CAD27 peptide can be cyclized by head-to-tail to form a secondary cyclic structure, which is linked by a disulfide bond between cysteine residues through cysteine 1-27. The cyclic engineering peptide presents several additional properties, such as the large surface area that provides a high affinity and selectivity for the targets, highly stable, lower immunogenicity and low toxicity, offering a promising approach to improve its biological activity[20, 21]. Our data show that synthetic CAD27 peptide treatment provided similar benefits in the inhibition of CNV formation compared to recombinant CAD protein (CAD112), suggesting that the chemically synthetic peptides did not alter its anti-angiogenic properties (Supplementary Figure 3). In addition, intravitreal and topical application of CAD27 also showed a similar inhibitory effect on the reduction of CNV lesions compared with Lucentis® (Ranibizumab), a standard treatment option for nAMD. Thus, these data make a compelling case that CAD27 delivered by intravitreal or topical application can be used as a therapeutic alternative to conventional therapies for pathologic ocular neovascularization.

 doi:10.20944/preprints201807.0347.v2

Intravitreal and topical routes were used to assess the therapeutic effect of CAD27 for the treatment of CNV. Intravitreal injection has been considered as an effective way to administer pharmacological treatments to the eye for managing pathological conditions associated with abnormal blood vessel growth, such as nAMD and diabetic retinopathy, and which requires frequent intravitreal injections for life. Nevertheless, retinal specialists are not easily accessible in regional communities, less developed or developing countries for intraocular injections that the diseases will eventually progress to blindness. Intravitreal injection also carries risks of potentially blinding complications and serious intraocular infections. Topical application of ophthalmic formulation, is the most convenient, safe, effective and less invasive drug delivery method, could potentially eliminate the risks of eye injections and increase the accessibility for patients. Several studies have previously demonstrated the feasibility of topical application of ophthalmic formulation for the management of CNV[22-25]. Therefore, in the present study, we have assessed the therapeutic potential of CAD27 on targeting CNV delivered via both intravitreal injection and topical application. Indeed, our data indicate both delivery routes provide similar benefits in reducing CNV lesions, suggesting that both the drug delivery methods are available and effectual in the rat laser-induced CNV model. These data are also consistent with our previous study that topical delivery of recombinant CAD proteins (CAD180 and 48) attenuates the development of CNV in the laser-induced CNV[14, 26, 27]. Moreover, CAD27 may have additional benefits than CAD180 or 48 as it can be chemically synthesized and low molecular weight that allows to have better retinal or trans-scleral penetration to the posterior segment when it is administered through intravitreal injection and topical application, respectively. Further research is needed to confirm its pharmacokinetic profile and bioavailability in the eye, particularly by topical administration. In addition, using *in vivo* ERG assessment, we showed that intravitreal or topical application of CAD27 had little effect on retinal function over the course of 14 days. However, the long-term safety of CAD27-based therapy will need to be confirmed before their translation into clinical trials.

In summary, our study demonstrates that therapeutic delivery of CAD27 attenuates the formation of CNV *in vivo*. Although further investigations are required to assess pharmacokinetic profile and long-term efficacy, our data suggest that topical application of CAD27 may be a viable therapeutic alternative for choroidal neovascularization, as it doesn't require ocular injection and can thus avoid the risks associated with the frequent injections required for current therapies.

4.Materials and methods

4.1.Site-directed mutagenesis

CAD48 cDNA was PCR from CAD and subcloned into the NdeI and XhoI sites of the pET32a(+) vector (catalog no. 69015, Novagen Inc., Madison, WI, USA) to yield the pET32a(+)-CAD48 plasmid (Supplementary information). Point mutations were introduced by PCR using the QuikChange Site-Directed Mutagenesis kit (catalog no. 200519, Agilent Technologies, Santa Clara, CA, USA) according to the manufacturer's instructions. The mutagenic oligonucleotide primers were designed using a web-based QuikChange Primer Design Program (www.agilent.com/genomics/qcpd) and are shown in Supplementary Table 1. PCRs for single amino acid mutations were run for 18 cycles of 30 seconds at 95 ℃, 1 minute at 55 ℃, and followed by 1 minute at 68 ℃. The resulting mutant plasmids were verified by DNA sequencing.

4.2. Expression and purification of recombinant TrxA-tagged truncated CAD protein

Recombinant TrxA-CAD was expressed and purified as previously described[7]. Briefly, pET32a(+)-CAD48 or mutant plasmid was transformed in BL21(DE3)pLysS Competent Cells (catalog no. 69451, Novagen Inc.) and the transformed cells were grown at 37 ℃ until log-phase (optical density [OD 600 nm] of 0.5-0.9). Expression of P protein was induced by addition of 1 mM isopropyl thiogalactose (IPTG; catalog no. I6758, Sigma-Aldrich, St. Louis, MO, USA) and the culture was incubated for additional 3 hours. The cell pellet was harvested by centrifugation at 5,000 rpm for 10 min at 4 ℃, resuspended in the binding buffer (20 mM phosphate buffer, pH 7.4, 20 mM imidazole,

 doi:10.20944/preprints201807.0347.v2

150 mM NaCl, 1 mM EDTA, 1 mM PMSF, 1 μg/ml aprotinin, 1 μg/ml leupeptin, and 1 μg/ml pepstatin), then homogenized by sonication. After centrifugation at 12,000 rpm for 20 min at 4 °C, the supernatant was mixed with Ni-NTA agarose (catalog no. 30210, Qiagen, Valencia, CA, USA) at 4 ℃ for 30 min. The beads were washed four times with the binding buffer, and the recombinant protein was eluted with buffer (20 mM phosphate buffer, pH 7.4, 250 mM imidazole, 150 mM NaCl). Salted and endotoxin were removed by passing through a G-25 Sephadex column (catalog no. 17085101, GE Healthcare Life Sciences, Pittsburgh, PA, USA) and Detoxi-G gel (catalog no. 88270, Pierce, Rockford, IL, USA).

4.3.Preparation of CAD27 peptide

CAD27 peptide (CGPGTKKVHVIFNYKGKNVLINKDIRC) and presumed non-functional form scrambled peptide (Csr27; CVKIGLRGNTVKPYKFNIKDHVGKNIC) were manufactured by de novo peptide synthesis (Kelowan Incs, Taipei, Taiwan). The synthesized peptides were reconstituted in Dulbecco's Phosphate Buffered Saline (DPBS; catalog no. 14190144, Gibco™, Invitrogen, Carlsbad, CA, USA) for *in vitro* and *in vivo* studies.

4.4.Cell culture

Human primary umbilical vein endothelial cell, HUVEC, was purchased from Lonza (catalog no. CC-2519; Walkersville, MD, USA) and cultured in endothelial cell basal medium-2 (EBM-2) supplemented with the EGM™-2 BulletKit™ (catalog no. CC-5035; Lonza) in a humidified 5% CO_2 at 37℃. Human endothelial cells line, EA.hy926, was purchased from ATCC (CRL-2922™) and cultured in Dulbecco's Modified Eagle's Medium (DMEM; catalog no. 11965118, Invitrogen) supplemented with Penicillin-Streptomycin (50 U/mL; catalog no. 15140122, Invitrogen), 10% fetal bovine serum (FBS; Gibco™, Invitrogen) and L-glutamine (2mM; catalog no. 25030081, Invitrogen) in a humidified 5% CO_2 at 37℃.

4.5.Tube formation assay

Quantification of tube formation was performed using a previously described method[26] . Briefly, 24-well plate was pre-incubated with BD Matrigel™ Basement Membrane Matrix (catalog no. 356234, BD Biosciences, Franklin Lakes, NJ, USA) at 37 ℃ for 30 minutes. Cells were incubated with DPBS, CAD27 (10 and 20 μg/mL), or Csr27 (10 and 20 μg/mL) at 37 ℃ for 5 hours. Cells (1.5×10^4) were re-suspended in the completed medium and loaded on the top of the Matrigel. Following a 6 hours incubation at 37 ℃, each well was photographed under a bright field phase contrast microscope. The numbers of endothelial tube lumens were counted in three replicate wells and only the completed ring structures created by 3 to 5 endothelial cells were considered as tubes. The analysis was performed in Image J version 1.48 software (http://imag ej.nih.gov/ij/; provided in the National Institutes of Health, Bethesda, MD, USA).

4.6.Cell migration assay

Cell migration was performed in a Boyden's chambers (catalog no. CBA-100-C, Cell Biolabs, INC, CA, USA), which comprising the upper and lower system separated by a 0.005 % gelatin coating 8-μm pore size polycarbonate membrane, as previously described[26]. Cells (2×10^4) were re-suspended in serum-free medium, loaded onto the upper well and incubated with vehicle (DPBS), CAD27 (10 and 20 μg/mL), or Csr27 (10 and 20 μg/mL), respectively, in a humidified 5% CO_2 at 37℃ for 6 hours. The cells on the upper side of the filter were removed. Those that had migrated to the lower side were fixed in absolute methanol, stained with 10 % Giemsa solution (Merck, Darmstadt, Germany) and five high power fields from each well were counted under a bright field phase contrast microscope (Olympus BX40; Olympus Optical Co., Tokyo, Japan).

 doi:10.20944/preprints201807.0347.v2

4.7.Aortic ring assay

This *ex vivo* aortic ring angiogenesis assay was performed as described previously[26] . Briefly, the thoracic aortas were excised from 3 week-old male Sprague-Dawley rats and immediately placed into prechilled DMEM containing 10% FBS. Clotted blood inside the aorta was flushed with media, and the peri-adventitial fibroadipose tissue was removed. Aortas were then cut into cross-sectional rings about 1-1.5 mm in length. Rings were placed into a 24-well plate containing 0.5 mL of cold BD Matrigel™ Basement Membrane Matrix supplemented with MCDB131 medium (catalog no. 10372019, Invitrogen) and incubated at 37 ℃ until the Matrigel polymerized. Subsequently, aortic rings were treated with vehicle (DPBS), CAD27 (10 μg/mL), or Csr27 (10 μg/mL) and maintained in a humidified 5 % CO_2 at 37℃ for 5 days. Microvascular sprouting from each aortic ring were examined and imaged daily under a bright field phase contrast microscope (Olympus BX40). The greatest distances from the aortic ring body to the end of the vascular sprouts (sprout length) were measured by Image J version 1.48 software at 3 distinct points per ring and in 3 different rings per treatment group.

4.8.Animal and ethical approval

All animals were handled in accordance with the ARVO Statement for the Use of Animals in Ophthalmic and Vision Research. for the experiments performed in this study was obtained from the Institutional Animal Care and Use Committee (IACUC) of Kaohsiung Veterans General Hospital. The pigmented Brown Norway rats (8 week-old, female) and Sprague-Dawley rats (3 week-old, male) were purchased from National Animal Center, Taipei, Taiwan. Rats were housed in standard cages, with free access to food and water in a temperature-controlled environment under a 12-h light (50 lux illumination) and 12-h dark (< 10 lux illumination) cycle to minimize possible light-induced damage to the eye.

4.9.Generation of CNV by laser photocoagulation

The CNV lesions were induced in rat eyes by laser photocoagulation as previously described[26]. Briefly, Brown Norway rats were anesthetized with an intramuscular injection of a mixture of 2% xylocaine (0.15 mL/kg body weight, Astra, Astra Sodertalje, Sweden) and ketamine (50 mg/kg body weight, Parke-Davis, Morris Plains, NJ, USA). Pupils were dilated with 1% tropicamide (Alcon Laboratories, Fort Worth, TX, USA). A piece of cover glasses was served as a contact lens to improve the visibility of the fundus. Argon laser (Novus Omni; Coherent, Palo Alto, CA, USA) irradiation was delivered through a slit lamp (Carl Zeiss, Oberkochen, Germany). Laser parameters were set as follows: spot size of 50 μm, power of 400 mW, and exposure duration of 0.05 second. Disruption of Bruch's membrane was detected by the emergence of a bubble at the center of photocoagulation in the laser spotted zone. Six lesions were generated in each eye at the 1, 3, 5, 7, 9 and 11 o'clock positions located at equal distances from the optic disk and between the major retinal vessels.

4.10.Intravitreal injection and topical application

One day after laser-induced CNV induction, rats were anesthetized with a combination of xylocaine (0.15 mL/kg body weight) and ketamine (50 mg/kg body weight). Intravitreal injection was performed under a surgical microscope as previously described[18] . After a small puncture through the conjunctiva and sclera was created using a 30 gauge needle, a 32 gauge blunt needle connected to a 10-μL Hamilton syringe was inserted into the vitreous and 5 μL of DPBS suspension containing Lucentis® (ranibizumab, 50 μg; Novartis, Basel, Switzerland), CAD27 (10 and 20 μg), or vehicle (DPBS) was injected into one eye of each rat using a UMP3-2 Ultra Micro Pump (World Precision Instruments, Sarasota, FL, USA) at a rate of 100 nL/s. Only a single injection was permed in the CNV rat. The CAD27 (10 and 20 μg/mL) were formulated as eye drop in DPBS and topical installed three times a day in the rat eye after CNV induction for 28 days.

4.11.Electroretinogram (ERG)

The single bright flash ERGs (UTAS-E 300; LKC Technology, Gaithersburg, MD) under a dark-adapted environment (~12 hours) were performed to assess the effect of intravitreal or topical administration of CAD 27 on retinal function. After at least 30 mins of darkness adaptation, rats were anesthetized. Gold foil was placed on the cornea with 2% methylcellulose gel (Omni Vision, Neuhausen, Switzerland). A reference electrode was attached to the shaven skin of the head and a ground electrode clipped to the rat's ear. After reducing the background noise below 60 Hz, a single flash of bright light (duration, 100 ms), 30 cm from the eye, was used as the light stimulus. Responses were amplified with a gain setting ±500 μV and filtered with low 0.3 Hz and high 500 Hz from an amplifier. Data were acquired, digitized, and analyzed using EM for Windows, version 2.6.

4.12.Fundus fluorescein angiography (FFA)

The size of CNV lesions were evaluated by FFA analysis using a digital fundus camera (Visupac 450, Ziess FF450, Germany) on day 24 after laser photocoagulation[28]. The rats were anaesthetized and the fluorescein sodium solution (10% Fluorescite; Alcon, Fort Worth, TX, USA) was intraperitoneally injected at a dose of 0.1 ml/kg body weight. Late-phase angiograms were obtained at 8 minutes after injection, and digital fundus pictures of bilateral eyes were taken within 1 minute. A choroidal neovascularization was defined as present when early hyper-fluorescence with late leakage was present at the site of laser injury[26]. The leakage of the CNV lesions were graded using leakage score system[29, 30]. Score 0 means no staining (no hyper-fluorescence), Score 1 means staining (hyper-fluorescence without leakage), Score 2 means moderate leakage (hyper-fluorescence in the early or midtransit images and late leakage), and Score 3 means heavy leakage (bright hyper-fluorescence in the transit images and late leakage beyond treated areas). The scores were assessed by two independent ophthalmologists who were masked to the experimental design.

4.13.Quantification of choroidal vascularity by flat-mounted analysis

Rats were euthanized 28 days after laser photocoagulation. The choroidal blood vessels in rat eyes were labeled by perfusion with fluorescein isothiocyanate (FITC)-dextran (2 x 10^6 MW; catalog no. FD2000S, Sigma-Aldrich, St. Louis, MO, USA)[31, 32]. Briefly, the rats were anaesthetized and subjected to an intracardiac perfusion of approximately 50 mL of lactated Ringer solution, followed by 20 mL of FITC-dextran in lactated Ringer solution (5 mg/mL) with gelatin (10%, w/v; catalog no. G9382, Sigma-Aldrich). The eyes were enucleated and fixed in 10% phosphate-buffered formalin for 2 hours at room temperature. After the cornea and lens were removed, the RPE/choroid/sclera flat-mounts were obtained on microscopic slides. Flat-mounts were imaged with a laser-scanning confocal fluorescence microscope. The areas of hyper-fluorescence associated with each CNV lesion was measured by observers who were blinded to the groups using ImageJ version 1.48 software.

4.14.Statistical Analysis

Results are presented as means ± standard errors of the means (SEM). The experimental data was analyzed with one-way ANOVA followed by Tukey's multiple comparisons test or two-tailed Student's t-test (GraphPad Prism software version 7.0). A value of *P* less than 0.05 was considered statistically significant.

Acknowledgements: This work was supported by grants from the Kaohsiung Veterans General Hospital (VGHKS 101-056, 103-089), The National Health and Medical Research Council of Australia (#1061912), The Ophthalmic Research Institute of Australia, and The Rebecca L. Cooper Medical Research Foundation.

Author Contributions: Conceptualization, Y.S.B., M.H.T. and G.S.L. Methodology, Y.S.B., H.H., M.H.T. and G.S.L. Formal Analysis, Y.S.B., J.C., P.J.T., M.H.T. and G.S.L. Investigation, Y.S.B., J.C. and P.J.T. Resources, Y.S.B., S.J.S., M.H.T. and G.S.L. Data Curation, Y.S.B., M.H.T. and G.S.L. Writing- Original Draft, Y.S.B., M.H.T. and G.S.L. Writing- Review & Editing, J.C., S.J.S., H.C.L. and H.H. Visualization, Y.S.B., J.C., M.H.T. and G.S.L.

Supervision, Y.S.B., M.H.T. and G.S.L. Project Administration, Y.S.B., M.H.T. and G.S.L. Funding Acquisition, Y.S.B. and M.H.T.

Conflicts of Interest: None of the authors have conflicts of interest to disclose.

References

1. Campochiaro, P. A., Retinal and choroidal neovascularization. *J.Cell Physiol* **2000,** 184, (3), 301-310.
2. Cheung, C. M. G.; Arnold, J. J.; Holz, F. G.; Park, K. H.; Lai, T. Y. Y.; Larsen, M.; Mitchell, P.; Ohno-Matsui, K.; Chen, S. J.; Wolf, S.; Wong, T. Y., Myopic Choroidal Neovascularization: Review, Guidance, and Consensus Statement on Management. *Ophthalmology* **2017,** 124, (11), 1690-1711.
3. Chan, W. M.; Lai, T. Y.; Liu, D. T.; Lam, D. S., Intravitreal bevacizumab (Avastin) for myopic choroidal neovascularization: six-month results of a prospective pilot study. *Ophthalmology* **2007,** 114, (12), 2190-6.
4. Ip, M. S.; Scott, I. U.; Brown, G. C.; Brown, M. M.; Ho, A. C.; Huang, S. S.; Recchia, F. M.; American Academy of, O., Anti-vascular endothelial growth factor pharmacotherapy for age-related macular degeneration: a report by the American Academy of Ophthalmology. *Ophthalmology* **2008,** 115, (10), 1837-46.
5. Pike, S. E.; Yao, L.; Jones, K. D.; Cherney, B.; Appella, E.; Sakaguchi, K.; Nakhasi, H.; Teruya-Feldstein, J.; Wirth, P.; Gupta, G.; Tosato, G., Vasostatin, a calreticulin fragment, inhibits angiogenesis and suppresses tumor growth. *The Journal of experimental medicine* **1998,** 188, (12), 2349-56.
6. Pike, S. E.; Yao, L.; Setsuda, J.; Jones, K. D.; Cherney, B.; Appella, E.; Sakaguchi, K.; Nakhasi, H.; Atreya, C. D.; Teruya-Feldstein, J.; Wirth, P.; Gupta, G.; Tosato, G., Calreticulin and calreticulin fragments are endothelial cell inhibitors that suppress tumor growth. *Blood* **1999,** 94, (7), 2461-8.
7. Wu, P. C.; Yang, L. C.; Kuo, H. K.; Huang, C. C.; Tsai, C. L.; Lin, P. R.; Wu, P. C.; Shin, S. J.; Tai, M. H., Inhibition of corneal angiogenesis by local application of vasostatin. *Molecular vision* **2005,** 11, 28-35.
8. Shu, Q.; Li, W.; Li, H.; Sun, G., Vasostatin inhibits VEGF-induced endothelial cell proliferation, tube formation and induces cell apoptosis under oxygen deprivation. *International journal of molecular sciences* **2014,** 15, (4), 6019-30.
9. Yao, L.; Pike, S. E.; Tosato, G., Laminin binding to the calreticulin fragment vasostatin regulates endothelial cell function. *Journal of leukocyte biology* **2002,** 71, (1), 47-53.
10. Huegel, R.; Velasco, P.; De la Luz Sierra, M.; Christophers, E.; Schroder, J. M.; Schwarz, T.; Tosato, G.; Lange-Asschenfeldt, B., Novel anti-inflammatory properties of the angiogenesis inhibitor vasostatin. *J Invest Dermatol* **2007,** 127, (1), 65-74.
11. Martin, D. F.; Maguire, M. G.; Ying, G. S.; Grunwald, J. E.; Fine, S. L.; Jaffe, G. J., Ranibizumab and bevacizumab for neovascular age-related macular degeneration. *N Engl J Med* **2011,** 364, (20), 1897-908.
12. Campochiaro, P. A.; Aiello, L. P.; Rosenfeld, P. J., Anti-Vascular Endothelial Growth Factor Agents in the Treatment of Retinal Disease: From Bench to Bedside. *Ophthalmology* **2016,** 123, (10S), S78-S88.
13. Prea, S. M.; Chan, E. C.; Dusting, G. J.; Vingrys, A. J.; Bui, B. V.; Liu, G. S., Gene Therapy with Endogenous Inhibitors of Angiogenesis for Neovascular Age-Related Macular Degeneration: Beyond Anti-VEGF Therapy. *J Ophthalmol* **2015,** 2015, 201726.
14. Sheu, S. J.; Chou, L. C.; Bee, Y. S.; Chen, J. F.; Lin, H. C.; Lin, P. R.; Lam, H. C.; Tai, M. H., Suppression of choroidal neovascularization by intramuscular polymer-based gene delivery of vasostatin. *Exp Eye Res* **2005,** 81, (6), 673-9.
15. Lange-Asschenfeldt, B.; Velasco, P.; Streit, M.; Hawighorst, T.; Pike, S. E.; Tosato, G.; Detmar, M., The angiogenesis inhibitor vasostatin does not impair wound healing at tumor-inhibiting doses. *J Invest Dermatol* **2001,** 117, (5), 1036-41.
16. O'Reilly, M. S.; Boehm, T.; Shing, Y.; Fukai, N.; Vasios, G.; Lane, W. S.; Flynn, E.; Birkhead, J. R.; Olsen, B. R.; Folkman, J., Endostatin: an endogenous inhibitor of angiogenesis and tumor growth. *Cell* **1997,** 88, (2), 277-85.
17. O'Reilly, M. S.; Holmgren, L.; Chen, C.; Folkman, J., Angiostatin induces and sustains dormancy of human primary tumors in mice. *Nat Med* **1996,** 2, (6), 689-92.

Tu, L.; Wang, J. H.; Barathi, V. A.; Prea, S. M.; He, Z.; Lee, J. H.; Bender, J.; King, A. E.; Logan, G. J.; Alexander, I. E.; Bee, Y. S.; Tai, M. H.; Dusting, G. J.; Bui, B. V.; Zhong, J.; Liu, G. S., AAV-mediated gene delivery of the calreticulin anti-angiogenic domain inhibits ocular neovascularization. *Angiogenesis* **2018,** 21, (1), 95-109.

Lee, J. H.; Wang, J. H.; Chen, J.; Li, F.; Edwards, T. L.; Hewitt, A. W.; Liu, G. S., Gene therapy for visual loss: Opportunities and concerns. *Prog Retin Eye Res* **2018**.

Wang, L.; Gagey-Eilstein, N.; Broussy, S.; Reille-Seroussi, M.; Huguenot, F.; Vidal, M.; Liu, W. Q., Design and synthesis of C-terminal modified cyclic peptides as VEGFR1 antagonists. *Molecules* **2014,** 19, (10), 15391-407.

Chan, L. Y.; Craik, D. J.; Daly, N. L., Dual-targeting anti-angiogenic cyclic peptides as potential drug leads for cancer therapy. *Sci Rep* **2016,** 6, 35347.

Birke, K.; Lipo, E.; Birke, M. T.; Kumar-Singh, R., Topical application of PPADS inhibits complement activation and choroidal neovascularization in a model of age-related macular degeneration. *PloS one* **2013,** 8, (10), e76766.

Cloutier, F.; Lawrence, M.; Goody, R.; Lamoureux, S.; Al-Mahmood, S.; Colin, S.; Ferry, A.; Conduzorgues, J. P.; Hadri, A.; Cursiefen, C.; Udaondo, P.; Viaud, E.; Thorin, E.; Chemtob, S., Antiangiogenic activity of aganirsen in nonhuman primate and rodent models of retinal neovascular disease after topical administration. *Investigative ophthalmology & visual science* **2012,** 53, (3), 1195-203.

Kiuchi, K.; Matsuoka, M.; Wu, J. C.; Lima e Silva, R.; Kengatharan, M.; Verghese, M.; Ueno, S.; Yokoi, K.; Khu, N. H.; Cooke, J. P.; Campochiaro, P. A., Mecamylamine suppresses Basal and nicotine-stimulated choroidal neovascularization. *Investigative ophthalmology & visual science* **2008,** 49, (4), 1705-11.

Robbie, S. J.; Lundh von Leithner, P.; Ju, M.; Lange, C. A.; King, A. G.; Adamson, P.; Lee, D.; Sychterz, C.; Coffey, P.; Ng, Y. S.; Bainbridge, J. W.; Shima, D. T., Assessing a novel depot delivery strategy for noninvasive administration of VEGF/PDGF RTK inhibitors for ocular neovascular disease. *Investigative ophthalmology & visual science* **2013,** 54, (2), 1490-500.

Bee, Y. S.; Sheu, S. J.; Ma, Y. L.; Lin, H. C.; Weng, W. T.; Kuo, H. M.; Hsu, H. C.; Tang, C. H.; Liou, J. C.; Tai, M. H., Topical application of recombinant calreticulin peptide, vasostatin 48, alleviates laser-induced choroidal neovascularization in rats. *Molecular vision* **2010,** 16, 756-67.

Wu, P. C.; Yang, L. C.; Kuo, H. K.; Huang, C. C.; Tsai, C. L.; Lin, P. R.; Shin, S. J.; Tai, M. H., Inhibition of corneal angiogenesis by local application of vasostatin. *Molecular vision* **2005,** 11, 28-35.

Sheu, S. J.; Chou, L. C.; Bee, Y. S.; Chen, J. F.; Lin, H. C.; Lin, P. R.; Lam, H. C.; Tai, M. H., Suppression of choroidal neovascularization by intramuscular polymer-based gene delivery of vasostatin. *Experimental Eye Research* **2005,** 81, (6), 673-679.

Rich, R. M.; Rosenfeld, P. J.; Puliafito, C. A.; Dubovy, S. R.; Davis, J. L.; Flynn, H. W., Jr.; Gonzalez, S.; Feuer, W. J.; Lin, R. C.; Lalwani, G. A.; Nguyen, J. K.; Kumar, G., Short-term safety and efficacy of intravitreal bevacizumab (Avastin) for neovascular age-related macular degeneration. *Retina* **2006,** 26, (5), 495-511.

Lai, C. C.; Wu, W. C.; Chen, S. L.; Xiao, X.; Tsai, T. C.; Huan, S. J.; Chen, T. L.; Tsai, R. J.; Tsao, Y. P., Suppression of choroidal neovascularization by adeno-associated virus vector expressing angiostatin. *Investigative ophthalmology & visual science* **2001,** 42, (10), 2401-7.

Edelman, J. L.; Castro, M. R., Quantitative image analysis of laser-induced choroidal neovascularization in rat. *Exp Eye Res* **2000,** 71, (5), 523-33.

Nambu, H.; Nambu, R.; Melia, M.; Campochiaro, P. A., Combretastatin A-4 phosphate suppresses development and induces regression of choroidal neovascularization. *Invest Ophthalmol.Vis.Sci.* **2003,** 44, (8), 3650-3655.

 doi:10.20944/preprints201807.0347.v2

485 **Table**

486 **Table 1.** The effect of intravitreal and topical application of CAD27 on retinal function assessed by ERG.

ERG parameters	Vehicle	Lucentis (IVI)	CAD27 (10μg, IVI)	CAD27 (20μg, IVI)	CAD27 (10μg/mL, TA)	CAD27 (20μg/mL, TA)	P value
a-wave amplitude, μV	-128.6±11.1	-145.7±10.9	-161.4±14.7	-142.1±10.2	-159.9±10.3	-163.3±9.2	0.1557
a-wave latency, ms	19.7±0.7	20.0±0.6	17.8±0.9	19.8±1.0	18.2±0.5	18.7±0.4	0.0834
b-wave amplitude μV	296.5±15.2	314.3±20.8	351.1±27.2	310.1±29.7	336.5±19.9	367.1±22.4	0.1522
b-wave latency, ms	58.7±1.5	55.1±1.4	51.9±2.2	52.2±2.5	54.8±1.5	54.2±1.3	0.0675

487 Statistical analysis was performed using one-way ANOVA.

488 IVI: intravitreal injection, TA: topical application.

489

490

491

 doi:10.20944/preprints201807.0347.v2

Supplementary Table 1. Mutagenic primers for site-directed mutagenesis.

Primer	Sequence
T174 FWD	5'-GAGTTTACACACCTGTACTAACTGATTGTGCGGCCAGAC-3'
T174 REV	5'-GTCTGGCCGCACAATCAGTTAGTACAGGTGTGTAAACTC-3'
D166 FWD	5'-CAAGGACATCCGTTGCAAGTAAGATGAGTTTACACACCTGT-3'
D166 REV	5'-ACAGGTGTGTAAACTCATCTTACTTGCAACGGATGTCCTTG-3'
I158 FWD	5'-GGCAAGAACGTGCTGTAAAACAAGGACATCCGTTGCAAGGATGATG-3'
I158 REV	5'-CATCATCCTTGCAACGGATGTCCTTGTTTTACAGCACGTTCTTGCC-3'
N150 FWD	5'-GAAGGTTCATGTCATCTTCTAATACAAGGGCAAGAACGTGC-3'
N150 REV	5'-GCACGTTCTTGCCCTTGTATTAGAAGATGACATGAACCTTC-3'
T142 FWD	5'-ATCTGTGGCCCTGGCTAAAAGAAGGTTCATGTCATCTTCAACTACAA-3'
T142 REV	5'-TTGTAGTTGAAGATGACATGAACCTTCTTTTAGCCAGGGCCACAGAT-3'

FWD: forward primer. REV: Reverse primer.

 doi:10.20944/preprints201807.0347.v2

508

509 **Figure Legend**

510 **Figure 1. The effect of truncated CAD on the inhibition of angiogenesis.** (A) Schematic
511 diagram of CAD and its truncated protein constructs. Five truncated CAD fragments derived from
512 CAD48 were generated by introducing a stop codon on each amino acid sequence of T141, N149,
513 I157, D165, and T173. CAD36 (residues C137-Y172) and CAD27 (residues C137-C163) were further
514 generated according to the functional motif of CAD and can form in a cyclic structure. N: N-terminal
515 domain. C: C-terminal domain. SP: Signal peptide. NF: Non-functional domain. AD: antiangiogenic
516 domain. (B) Amino acid sequence of TrxA-CAD recombinant proteins. The yellow square box
517 indicates truncated CAD fragments. *stop codon. (C) Purification and SDS-PAGE analysis of the
518 recombinant fragments of truncated CAD. (D) Effects of the CAD48 and its fragments on migration
519 of HUVECs. The quantification of migration assay characterizing migrated cells and data are
520 presented as the mean ± SEM (n=3). Statistical analysis between groups was performed using one-
521 way ANOVA followed by Tukey's multiple comparisons test (*$p < 0.05$, **$p < 0.001$, ***$p < 0.0001$).
522

523 **Figure 2. The effect of CAD27 on *in vitro* angiogenic activities.** (A) Schematic representation
524 of CAD27. CAD27 was derived from anti-angiogenic domain (residues 137-163) of calreticulin. N: N-
525 terminal domain. C: C-terminal domain. SP: Signal peptide. NF: Non-functional domain. AD:
526 antiangiogenic domain. (B) and (C) Effect of CAD27 on tube formation and migration in human
527 endothelial cells (EA.hy926) was assessed. (B) Representative images and quantitative analysis of
528 tube formation assay characterizing the lumen formation, and data are presented as the mean ± SEM
529 (n=4). Scale bar: 100μm. (C) Representative images and quantification of migration assay
530 characterizing migrated cells, and data are presented as the mean ± SEM (n=3-4). Statistical analysis
531 between groups was performed using one-way ANOVA followed by Tukey's multiple comparisons
532 test (**$p < 0.001$). Scale bar: 100μm.
533

534 **Figure 3. The effect of CAD27 on vascular sprouting from rat aortic ring explants.** (A)
535 Representative images and (B) quantitative analysis of vascular sprouting in 3 week-old rat aortic
536 ring explants. Data are presented as the mean ± SEM (n=5). Statistical analysis between groups was
537 performed using one-way ANOVA followed by Tukey's multiple comparisons test (**$p < 0.001$). Red
538 lines indicated the border zone of vascular sprouting.
539

540 **Figure 4. Fluorescein angiographic analysis of CNV lesions after an intravitreal or daily**
541 **topical application of CAD27.** (A) A schematic diagram of the timeline for the laser-induced CNV
542 rat model, treatments and examination. Retinal function was assessed by ERG (on day14). Choroidal
543 vascularity of laser-induced CNV lesions was examined by FFA (on day 24) and choroidal flat-mount
544 labeling with FITC-dextran (on day 28) after a single intravitreal injection or daily topical application
545 of CAD27. (B) Representative CNV lesions in rat eyes were identified by fundus fluorescein
546 angiography after an intravitreal or daily topical application of CAD27. (C) CNV lesions from
547 fluorescein angiography were analyzed at days 24 after treatment, and data are presented as
548 percentage of CNV score (n=26-46 from 6-8 eyes). Yellow arrows indicated the lesions of CNV. Lu:
549 Lucentis, IVI: intravitreal injection, TA: topical application.
550

551 **Figure 5. Flat-mount analysis of choroidal vascularity after an intravitreal or daily topical**
552 **application of CAD27.** Choroidal vascularity of laser-induced CNV lesions was examined by
553 labeling using FITC-dextran. (A) Representative profile of FITC-dextran-positive blood vessels in
554 choroidal flat-mounts at day 28 after treatment. Scale bar: 200μm. (B) FITC-dextran labeling CNV in
555 the choroidal flat-mounts was quantified and data are presented as mean ± SEM (n=26-31 from 6-8
556 eyes). Statistical analysis between groups was performed using two-tailed Student's t-test (*$p < 0.05$,
557 **$p < 0.001$, ***$p < 0.0001$). Red lines indicated the lesions of CNV in choroid flat-mount. Lu: Lucentis,
558 IVI: intravitreal injection, TA: topical application.

 doi:10.20944/preprints201807.0347.v2

559
560 **Supplementary Figure 1. The effect of intravitreal and topical application of CAD27 on retinal**
561 **function.** (A) Schematic representation of ERG waveforms at selected intensities from control (vehicle
562 injected eye). (B) Group of averaged ERG waveforms (a-wave amplitude, μV; b-wave amplitude, μV;
563 a-wave latency, ms; and b-wave latency, ms). Statistical analysis between groups was performed
564 using one-way ANOVA followed by Tukey's multiple comparisons test.
565
566 **Supplementary Figure 2. The original images of the choroidal vascularity of laser-induced**
567 **CNV lesions used in Figure 5A.** The area with the red dashed line indicates CNV lesion.
568
569 **Supplementary Figure 3. Flat-mount analysis of choroidal vascularity after an intravitreal**
570 **application of CAD112 and CAD27.** Choroidal vascularity of laser-induced CNV lesions was
571 examined by labeling using FITC-dextran. FITC-dextran labeling CNV in the choroidal flat-mounts
572 was quantified and data are presented as mean ± SD (n=6 eyes). CAD112 (10μg/5μL), CAD27
573 (20μg/5μL). using one-way ANOVA followed by Tukey's multiple comparisons test. (*$p < 0.01$).
574

Preprints (www.preprints.org) | NOT PEER-REVIEWED | Posted: 18 September 2018 doi:10.20944/preprints201807.0347.v2

575

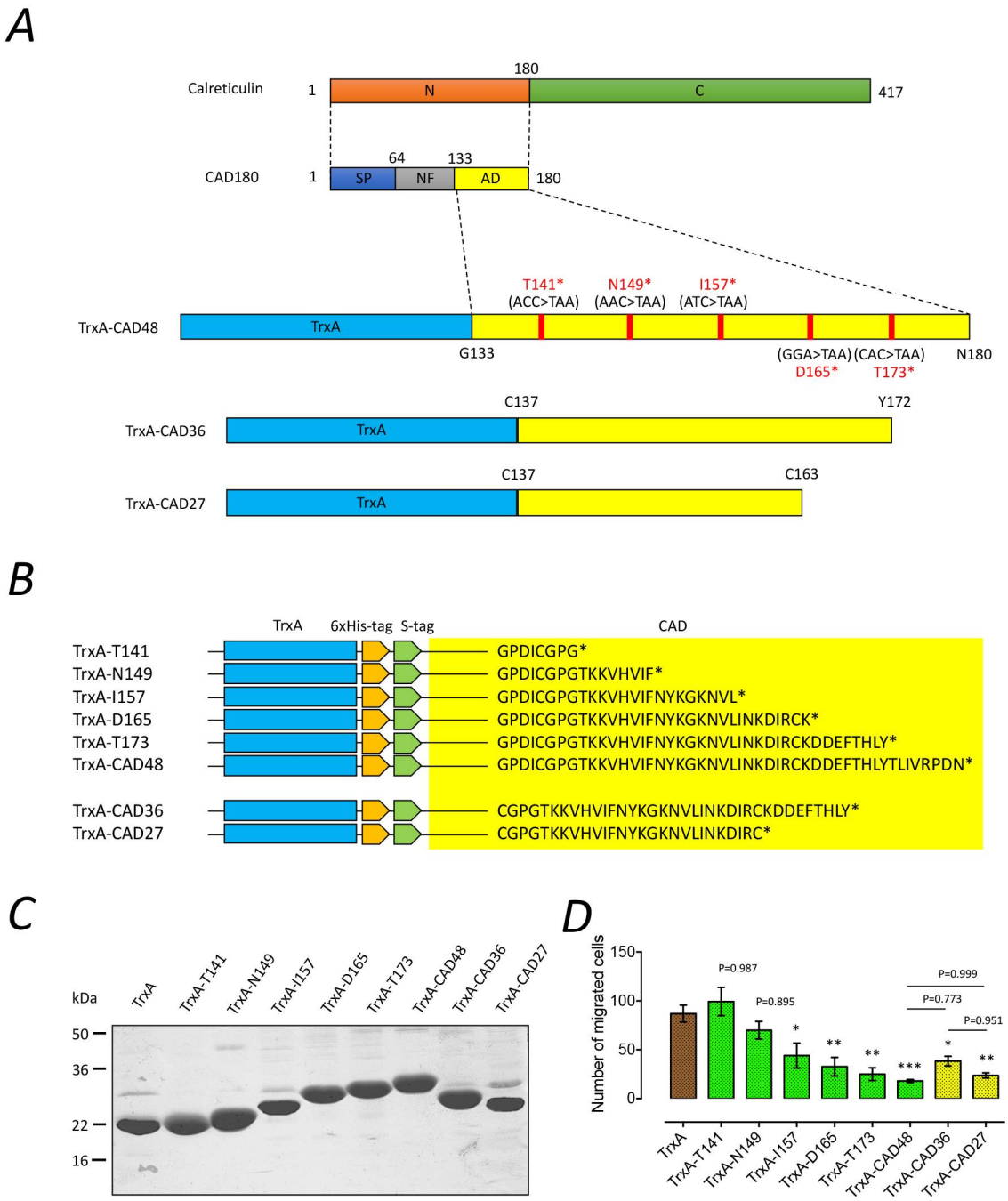

576

577 **Figure 1. The effect of truncated CAD on the inhibition of angiogenesis.** (A) Schematic diagram of CAD and
578 its truncated protein constructs. Five truncated CAD fragments derived from CAD48 were generated by
579 introducing a stop codon on each amino acid sequence of T141, N149, I157, D165, and T173. CAD36 (residues
580 C137-Y172) and CAD27 (residues C137-C163) were further generated according to the functional motif of CAD48
581 and can form in a cyclic structure. N: N-terminal domain. C: C-terminal domain. SP: Signal peptide. NF: Non-
582 functional domain. AD: antiangiogenic domain. (B) Amino acid sequence of TrxA-CAD recombinant proteins.
583 The yellow square box indicates truncated CAD fragments. *stop codon. (C) Purification and SDS-PAGE analysis
584 of the recombinant fragments of truncated CAD. (D) Effects of the CAD48 and its fragments on migration of
585 HUVECs. The quantification of migration assay characterizing migrated cells and data are presented as the mean
586 ± SEM (n=3). Statistical analysis between groups was performed using one-way ANOVA followed by Tukey's
587 multiple comparisons test ((*p < 0.05, **p < 0.001, ***p < 0.0001).

588

Preprints (www.preprints.org) | NOT PEER-REVIEWED | Posted: 18 September 2018 doi:10.20944/preprints201807.0347.v2

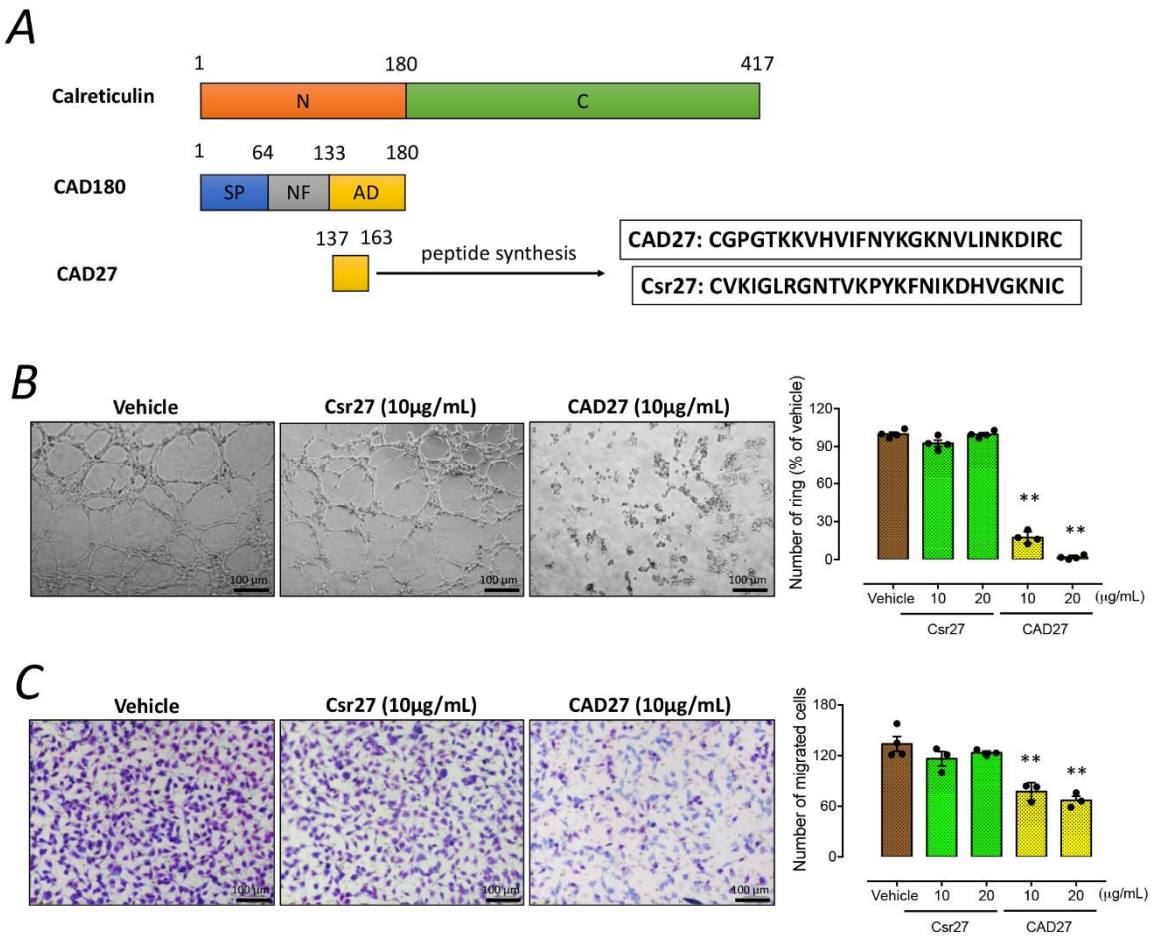

Figure 2. The effect of CAD27 on *in vitro* angiogenic activities. (A) Schematic representation of CAD27. CAD27 was derived from anti-angiogenic domain (residues 137-163) of calreticulin. N: N-terminal domain. C: C-terminal domain. SP: Signal peptide. NF: Non-functional domain. AD: antiangiogenic domain. (B) and (C) Effect of CAD27 on tube formation and migration in human endothelial cells (EA.hy926) was assessed. (B) Representative images and quantitative analysis of tube formation assay characterizing the lumen formation, and data are presented as the mean ± SEM (n=4). Scale bar: 100μm. (C) Representative images and quantification of migration assay characterizing migrated cells, and data are presented as the mean ± SEM (n=3-4). Statistical analysis between groups was performed using one-way ANOVA followed by Tukey's multiple comparisons test (**$p < 0.001$). Scale bar: 100μm.

Preprints (www.preprints.org) | NOT PEER-REVIEWED | Posted: 18 September 2018 doi:10.20944/preprints201807.0347.v2

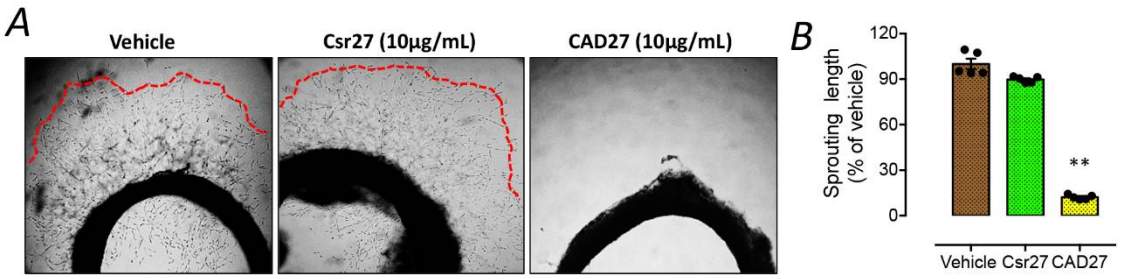

602

603 **Figure 3. The effect of CAD27 on vascular sprouting from rat aortic ring explants.** (A) Representative images
604 and (B) quantitative analysis of vascular sprouting in 3 week-old rat aortic ring explants. Data are presented as
605 the mean ± SEM (n=5). Statistical analysis between groups was performed using one-way ANOVA followed by
606 Tukey's multiple comparisons test (**$p < 0.001$). Red lines indicated the border zone of vascular sprouting.

607

Preprints (www.preprints.org) | NOT PEER-REVIEWED | Posted: 18 September 2018 doi:10.20944/preprints201807.0347.v2

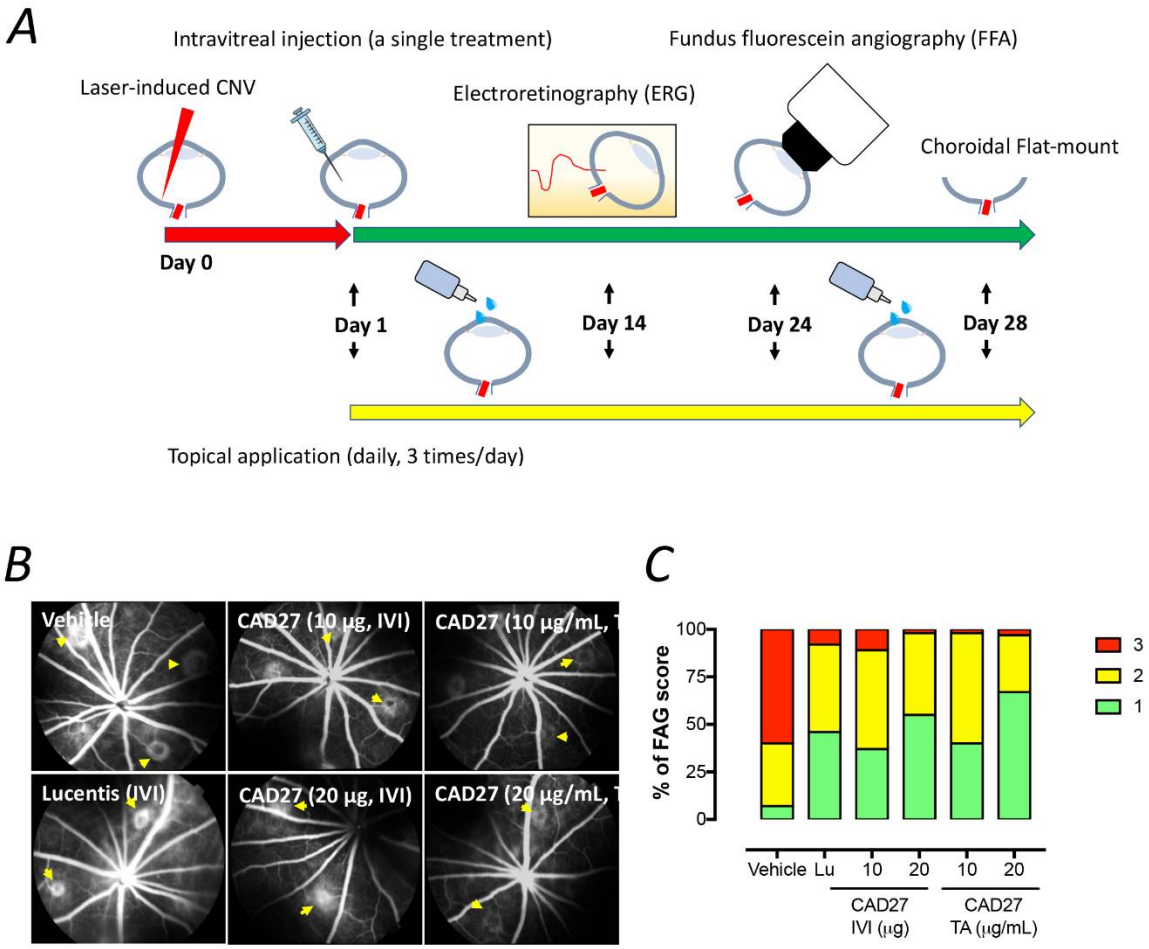

Figure 4. Fluorescein angiographic analysis of CNV lesions after an intravitreal or daily topical application of CAD27. (A) A schematic diagram of the timeline for the laser-induced CNV rat model, treatments and examination. Choroidal vascularity of laser-induced CNV lesions was examined by FFA (day 24) and choroidal flat-mount labeling with FITC-dextran (day 28) after a single intravitreal injection or daily topical application of CAD27. (B) Representative CNV lesions in rat eyes were identified by fundus fluorescein angiography after an intravitreal or daily topical application of CAD27. (C) CNV lesions from fluorescein angiography were analyzed at days 24 after treatment, and data are presented as percentage of CNV score (n=26-46 from 6-8 eyes). Yellow arrows indicated the lesions of CNV. Lu: Lucentis, IVI: intravitreal injection, TA: topical application.

.

Preprints (www.preprints.org) | NOT PEER-REVIEWED | Posted: 18 September 2018 doi:10.20944/preprints201807.0347.v2

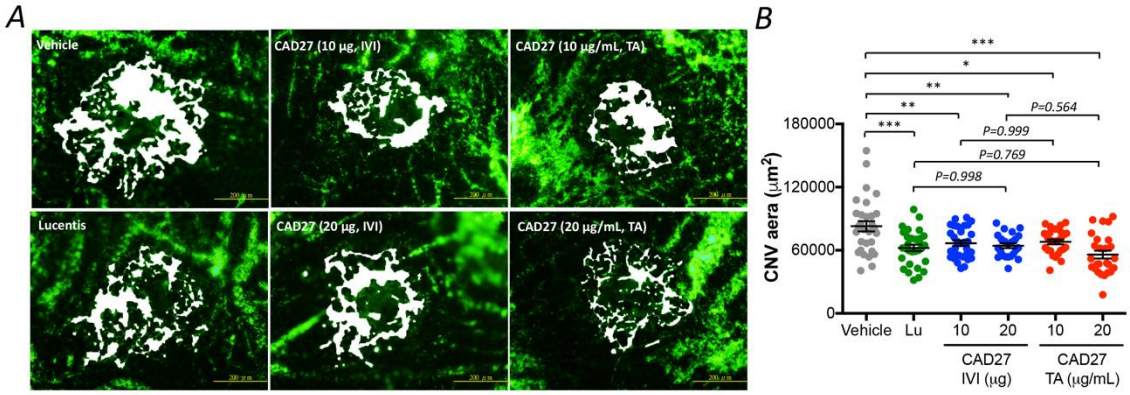

Figure 5. Flat-mount analysis of choroidal vascularity after an intravitreal or daily topical application of CAD27. Choroidal vascularity of laser-induced CNV lesions was examined by labeling using FITC-dextran. (A) Representative profile of FITC-dextran-positive blood vessels in choroidal flat-mounts at day 28 after treatment. Scale bar: 200μm. (B) FITC-dextran labeling CNV in the choroidal flat-mounts was quantified and data are presented as mean ± SEM (n=26-31 from 6-8 eyes using one-way ANOVA followed by Tukey's multiple comparisons test (*$p < 0.05$, **$p < 0.001$, ***$p < 0.0001$). Red lines indicated the lesions of CNV in choroid flat-mount. Lu: Lucentis, IVI: intravitreal injection, TA: topical application.

Preprints (www.preprints.org) | NOT PEER-REVIEWED | Posted: 18 September 2018 doi:10.20944/preprints201807.0347.v2

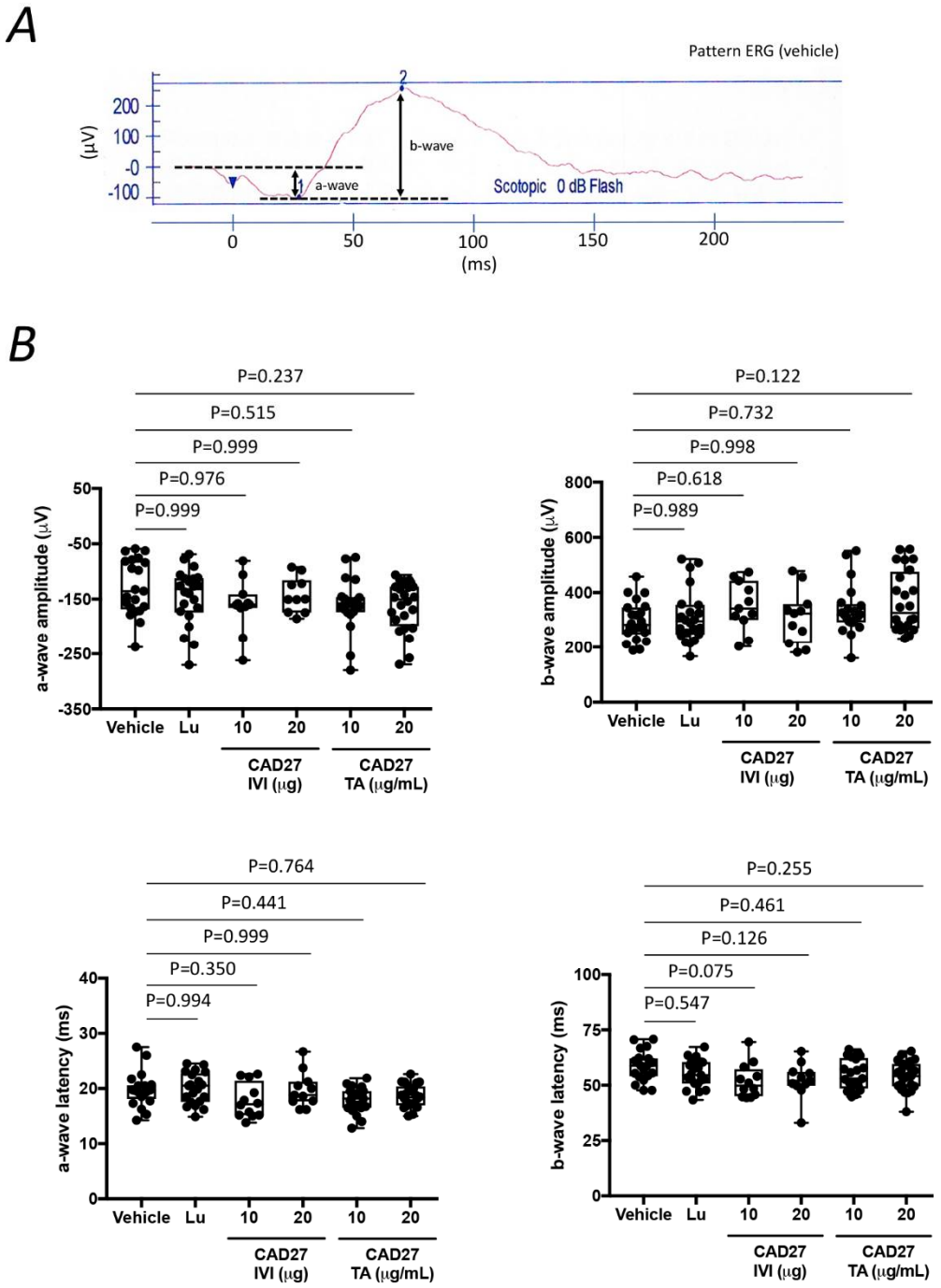

Supplementary Figure 1. The effect of intravitreal and topical application of CAD27 on retinal function. (A) Schematic representation of ERG waveforms at selected intensities from control (vehicle injected eye). (B) Group of averaged ERG waveforms (a-wave amplitude, μV; b-wave amplitude, μV; a-wave latency, ms; and b-wave latency, ms). Statistical analysis between groups was performed using one-way ANOVA followed by Tukey's multiple comparisons test.

Preprints (www.preprints.org) | NOT PEER-REVIEWED | Posted: 18 September 2018 doi:10.20944/preprints201807.0347.v2

636

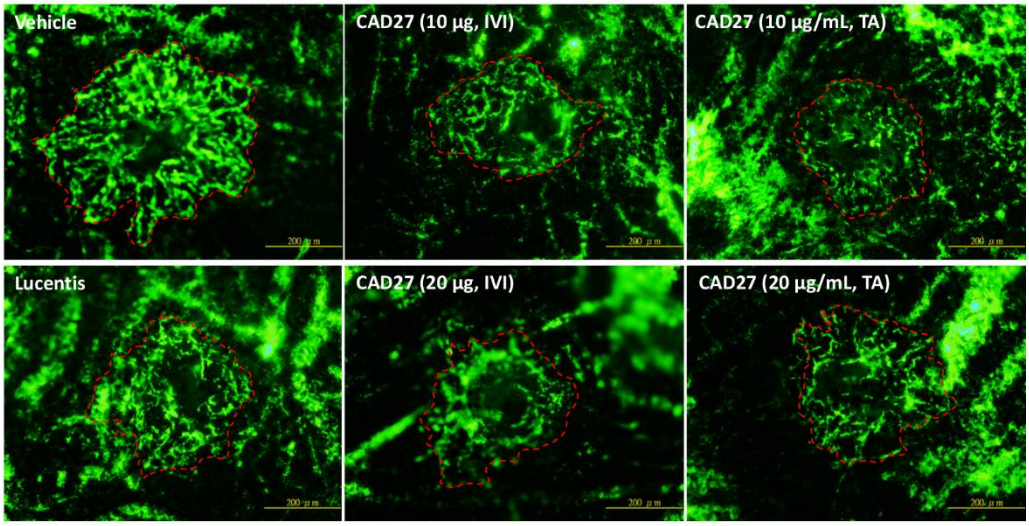

637

638 **Supplementary Figure 2. The original images of the choroidal vascularity of laser-induced CNV lesions used**
639 **in Figure 5A.** The area with the red dashed line indicates CNV lesion. Scale bar: 200μm.

640

641

Preprints (www.preprints.org) | NOT PEER-REVIEWED | Posted: 18 September 2018 doi:10.20944/preprints201807.0347.v2

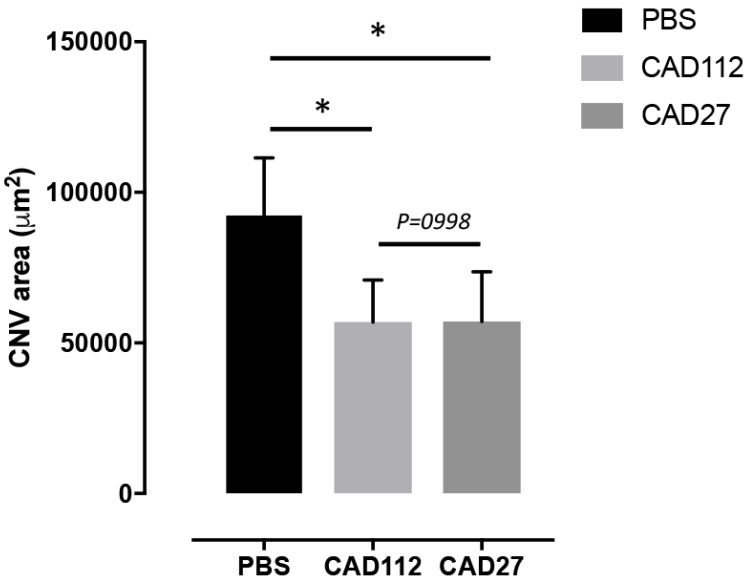

642
643 **Supplementary Figure 3. Flat-mount analysis of choroidal vascularity after an intravitreal application of**
644 **CAD112 and CAD27.** Choroidal vascularity of laser-induced CNV lesions was examined by labeling using FITC-
645 dextran. FITC-dextran labeling CNV in the choroidal flat-mounts was quantified and data are presented as mean
646 ± SD (n=6 eyes). CAD112 (10μg/5μL), CAD27 (20μg/5μL). using one-way ANOVA followed by Tukey's multiple
647 comparisons test. (*$p < 0.01$).

648